Photochemical & Photobiological Sciences

Accepted Manuscript

This is an *Accepted Manuscript*, which has been through the Royal Society of Chemistry peer review process and has been accepted for publication.

Accepted Manuscripts are published online shortly after acceptance, before technical editing, formatting and proof reading. Using this free service, authors can make their results available to the community, in citable form, before we publish the edited article. We will replace this *Accepted Manuscript* with the edited and formatted *Advance Article* as soon as it is available.

You can find more information about *Accepted Manuscripts* in the Information for Authors.

Please note that technical editing may introduce minor changes to the text and/or graphics, which may alter content. The journal's standard Terms & Conditions and the Ethical guidelines still apply. In no event shall the Royal Society of Chemistry be held responsible for any errors or omissions in this *Accepted Manuscript* or any consequences arising from the use of any information it contains.

ROYAL SOCIETY OF CHEMISTRY

www.rsc.org/pps

Protein-Encapsulated Bilirubin: Paving the Way to a Useful Probe for Singlet Oxygen

Frederico M. Pimenta,[a] Jan K. Jensen[b] Michael Etzerodt[b] and Peter R. Ogilby[a]*

[a] Center for Oxygen Microscopy and Imaging, Chemistry Department, Aarhus University, DK-8000, Aarhus, Denmark

[b] Department of Molecular Biology and Genetics, Aarhus University, DK-8000, Aarhus, Denmark

* To whom correspondence should be addressed: progilby@chem.au.dk

ABSTRACT

When dissolved in a bulk solvent, bilirubin efficiently removes singlet molecular oxygen, $O_2(a^1\Delta_g)$, through a combination of chemical reactions and by promoting the $O_2(a^1\Delta_g) \rightarrow O_2(X^3\Sigma_g^-)$ nonradiative transition to populate the ground state of oxygen. To elucidate how such processes can be exploited in the development of a biologically useful fluorescent probe for $O_2(a^1\Delta_g)$, pertinent photophysical and photochemical parameters of bilirubin encapsulated in a protein were determined. The motivation for studying a protein-encapsulated system reflects the ultimate desire to (a) use genetic engineering to localize the probe at a specific location in a living cell, and (b) provide a controlled environment around the chromophore/fluorophore. Surprisingly, explicit values of oxygen- and $O_2(a^1\Delta_g)$-dependent parameters that characterize the behavior of a given chromophore/fluorophore encased in a protein are not generally available. To the end of quantifying the effects of such an encasing protein, a recently discovered bilirubin-binding protein isolated from a Japanese eel was used. The data show that this system indeed preferentially responds to $O_2(a^1\Delta_g)$ and not to the superoxide ion. However, this protein not only shields bilirubin such that the rate constants for interaction with $O_2(a^1\Delta_g)$ decrease relative to what is observed in a bulk solvent, but the fraction of the total $O_2(a^1\Delta_g)$-bilirubin interaction that results in a chemical reaction between $O_2(a^1\Delta_g)$ and bilirubin also decreases appreciably. The rate constants thus obtained provide a useful starting point for the general design and development of reactive protein-encased fluorescent probes for $O_2(a^1\Delta_g)$.

INTRODUCTION

It is acknowledged that reactive oxygen species (ROS) play an important role in maintaining cell homeostasis and in the signaling events that occur as a result of a perturbation of the cell.[1-5] As such, there continues to be an extensive effort to develop fluorescent molecules that can selectively detect a given ROS under a wide range of conditions in living systems.[6-10] Of particular interest in this regard are protein-encased fluorescent probes that can be localized in a specific cellular domain through genetic engineering.[11, 12]

We have long been interested in one particular ROS: the lowest energy excited electronic state of molecular oxygen, singlet oxygen, $O_2(a^1\Delta_g)$.[13] As with other ROS (*e.g.*, the superoxide ion, H_2O_2, the hydroxyl radical), $O_2(a^1\Delta_g)$ has been implicated as an important intermediate in biological processes that range from cell death (apoptosis and necrosis) to cell proliferation (stimulated mitosis).[13-16]

Unlike other ROS, $O_2(a^1\Delta_g)$ has the unique feature that it can be directly and selectively monitored via its characteristic 1275 nm $O_2(a^1\Delta_g) \rightarrow O_2(X^3\Sigma_g^-)$ phosphorescence in time-resolved experiments, including those performed at the level of a single cell.[13, 17, 18] Nevertheless, these experiments are not trivial and are generally performed under special conditions that facilitate the detection of this weak optical signal.[13] Thus, there is a significant incentive to develop biologically compatible fluorescent molecules that selectively respond to the presence of $O_2(a^1\Delta_g)$ with a corresponding change in their fluorescence spectra. The use of a genetically-encoded probe is certainly a good way to achieve the goal of spatial localization in or on a cell. Carrying this latter point further, a protein-encased probe has the added advantage that its local environment, and hence its photochemistry and photophysics, will always be the same, irrespective of where in a cell it is placed.

Although there has been a reasonable effort dedicated to the design, development and characterization of discrete molecular probes for $O_2(a^1\Delta_g)$,[19-25] the study of genetically-encodable systems that are selective for $O_2(a^1\Delta_g)$ has lagged. In our view, the further development of such systems is limited by the lack of kinetic and photophysical data that characterizes and quantifies the general $O_2(a^1\Delta_g)$-relevant behavior of protein-encased chromophores/fluorophores.

In mechanistic studies to investigate the behavior of $O_2(a^1\Delta_g)$, it is often useful to add a molecule that can selectively quench or deactivate $O_2(a^1\Delta_g)$. In bulk solution phase systems, the molecules often used in this regard are sodium azide and 1,4-diazabicyclo[2.2.2]octane (DABCO), both of which efficiently promote the $O_2(a^1\Delta_g) \rightarrow O_2(X^3\Sigma_g^-)$ non-radiative transition.[26, 27] Alternatively, the well-known H_2O/D_2O solvent isotope effect on the lifetime of $O_2(a^1\Delta_g)$ can be used in this same way.[13, 26] For functioning biological systems such as a living cell there is great incentive to develop an analogous $O_2(a^1\Delta_g)$-perturbing system that can be specifically localized in a given intracellular spatial domain. To this end, a genetically-encodable system that selectively deactivates $O_2(a^1\Delta_g)$ will likewise be quite useful in a way that complements the fluorescent $O_2(a^1\Delta_g)$ probe described above.

With these points in mind, and with the desire to establish a useful quantitative framework for discussions of protein-based $O_2(a^1\Delta_g)$ probes, we set out to capitalize on a recent report describing the isolation and characterization of a bilirubin-binding protein isolated from a Japanese freshwater eel (*Anguilla japonica*).[28] The Japanese word for this freshwater eel, unagi, is well known to those who patronize sushi bars worldwide and was used to derive the moniker for this protein: UnaG.[28] Structures for both bilirubin and the UnaG-encased bilirubin are shown in Figure 1.

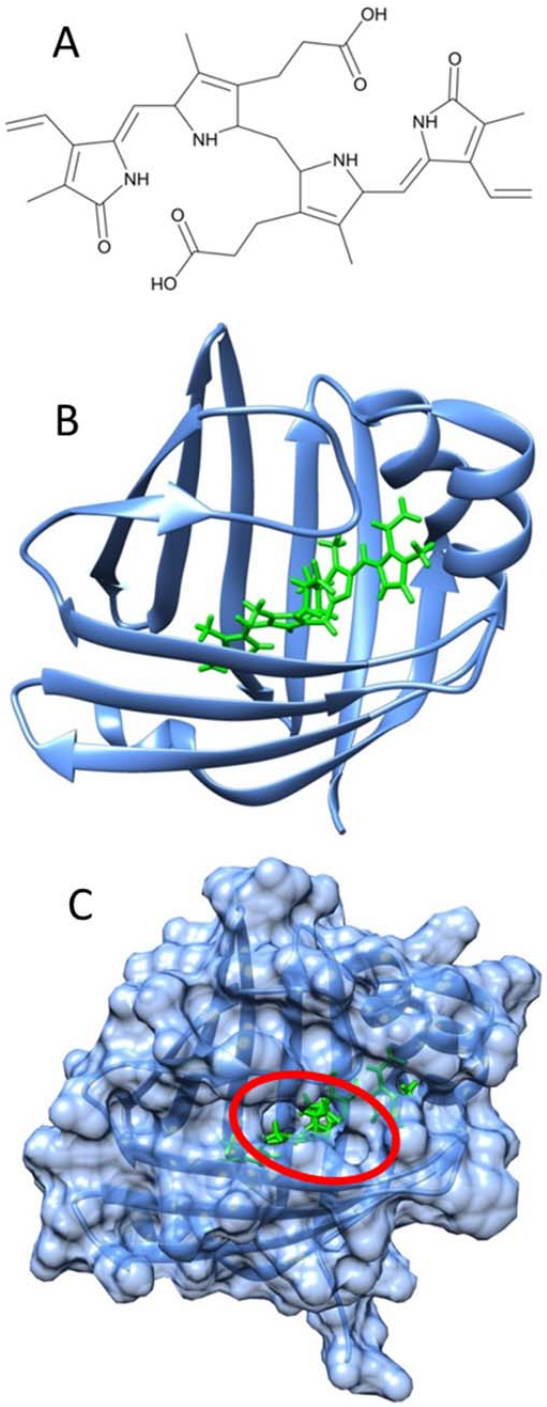

Figure 1. (A) Bilirubin drawn in a conformation that allows for favorable intramolecular hydrogen-bonding. (B) Illustration of the UnaG-encased bilirubin, where bilirubin is shown in green. (C) Corresponding illustration of the UnaG-encased bilirubin that also shows the van der Waals surface of the protein and the entry channel (red circle) through which externally-produced $O_2(a^1\Delta_g)$ must diffuse to encounter bilirubin. The latter illustrations are derived from the crystal structure reported for *holo*UnaG.[28]

The photochemistry and photophysics of bilirubin has long drawn the attention of the scientific community, principally given the accepted photodynamic treatment for neonatal jaundice which is characterized by locally high concentrations of bilirubin in lipophilic domains of the body (*i.e.*, photolysis renders the bilirubin more hydrophilic which, in turn, is more readily excreted by the body).[29, 30] Of particular relevance to the present study are reports that bilirubin efficiently removes $O_2(a^1\Delta_g)$ from bulk solvents (*i.e.*, chloroform, ethanol/D_2O) with an overall rate constant in the range 2-3 × 10^9 s^{-1} M^{-1} (*i.e.*, rate constant for the sum of the reactive and non-reactive channels for $O_2(a^1\Delta_g)$ removal).[31, 32] The rate constant for the $O_2(a^1\Delta_g)$-mediated decomposition of bilirubin that results in a loss of bilirubin fluorescence (*i.e.*, reactive $O_2(a^1\Delta_g)$ removal) was determined to be 4 × 10^8 s^{-1} M^{-1} in chloroform.[31] These data from bulk solvents are consistent with the known antioxidant properties of bilirubin in mammalian systems.[33] Moreover, the quantum yield of bilirubin fluorescence has been reported to increase from ~ 10^{-3} for the free solvated molecule to ~ 0.5 for the UnaG-encased molecule.[28, 34] Thus, this information bodes well for the potential use of UnaG-encased bilirubin as a model to better elucidate selected kinetic and photophysical aspects pertinent for the development of a protein-based probe for $O_2(a^1\Delta_g)$ that can also locally perturb $O_2(a^1\Delta_g)$ concentrations and thereby alter cell response to the production of $O_2(a^1\Delta_g)$.

From a practical perspective, given that bilirubin is endogenously produced by many mammalian cells, this protein-dependent $O_2(a^1\Delta_g)$ probe could be readily generated without the external addition of a chromophore/fluorophore. Indeed, the dissociation constant reported for UnaG-encapsulated bilirubin is quite small (K_D = 98 pM) indicating efficient noncovalent binding.[28] Thus, it is likely that one could indeed discriminate between the ambient and protein-bound intracellular populations of bilirubin. Carrying this latter point

further, we note that protein-encased biliverdin has recently been used as a $O_2(a^1\Delta_g)$ probe in cell experiments.[35] Biliverdin is an oxidized form of bilirubin (*i.e.*, hydrogenation/reduction of a double bond in biliverdin yields bilirubin[33]). Although this bodes well as a specific practical example, pertinent rate constants and photophysical parameters were not determined for the biliverdin system,[35] only increasing the relevance of our present study on protein-encapsulated bilirubin.

We therefore set out to characterize and quantify selected aspects of the interaction between bilirubin and $O_2(a^1\Delta_g)$, focusing on the effects that encapsulation of bilirubin in the UnaG protein have on this interaction.

EXPERIMENTAL SECTION

Chemicals. 9,10-Anthracenediyl-bis(methylene)dimalonic acid (ADA) (Fluka), Aluminum (III) phthalocyanine tetrasulfonic acid ($AlPcS_4$) (Frontier Scientific), potassium superoxide (Sigma Aldrich), and D_2O (> 99.9% D, Euriso-Top) were used as received. Bovine Serum Album (BSA) fraction V crystalline (≥ 99%) was obtained from Merck Millipore, while BSA fatty-acid free (≥ 99%), Human Serum Albumin (HSA) (≥ 97%), HSA fatty-acid free (≥ 96%), and Rat Serum Albumin (RSA) (≥ 99%) were obtained from Sigma-Aldrich and used as received.

The D_2O-based phosphate buffer was prepared by dissolving one PBS tablet (Sigma-Aldrich) in 200 mL of D_2O to yield a 10 mM phosphate buffer solution with 2.7 mM KCl and 137 mM NaCl at pD 7.8. The D_2O-based citrate (20 mM, pD 6.4) and N-cyclohexyl-3-aminopropanesulfonic acid, CAPS, (5 or 50 mM, pD 10.7) buffer solutions were prepared using the respective powders obtained from Sigma-Aldrich. (Note: pD = pH + 0.4)

Expression and Purification of UnaG. The UnaG plasmid was obtained as a gift from A. Miyawaki (RIKEN Brain Science Institute, Wako-City, Japan). The sequence encoding the UnaG protein, inserted in the vector pGEX-2T, was transferred to a pT_7 vector[36] as a fusion protein containing ubiquitin (UB) preceded by a six Histidine tag (H_6) and a Factor Xa cleavage site (FXa) between UB and UnaG. The new plasmid T_7H_6-UB-FXa UnaG was transformed into competent E. coli BL21 AI cells (Invitrogen), plated on 2xTYE-agar plates containing carbenicillin (100 μg mL^{-1}) and grown overnight. The UB-UnaG fusion protein was expressed in the dark from a single colony in 2xTYE medium supplemented with carbenicillin (100 μg mL^{-1}). Expression was induced by addition of arabinose to 0.2% w/v. Cells were harvested after 4 h of expression and lysed by sonication in 50 mM Tris–HCl (pH 8), 500 mM NaCl, 25 mM imidazole and a cocktail of protease inhibitors (Sigma-Aldrich). The insoluble protein extract was collected by centrifugation, resuspended in the same buffer supplemented with 4M Urea. The soluble extract was loaded into a Sephadex G-25 column (GE-Healthcare) to remove urea. Fractions containing the fusion protein were digested with FXa (100:1 w/w) for ~ 48 h at 30 °C, after which ~ 80% of the fusion protein was cleaved, as observed by SDS-PAGE. The digestion mixture was loaded into a Ni-NTA agarose column (Qiagen) to remove all ubiquitin and non-cleaved fusion protein and thereafter onto a benzamidine-Sepharose 6B CL column (GE HealthCare) to remove FXa. The UnaG protein eluted in the flow-through fraction from the columns in 50 mM Tris–HCl (pH 8), 500 mM NaCl, 25 mM imidazole. Samples were concentrated using a 50 mL AMICON stirred ultrafiltration cell equipped with a 10 kDa cut-off membrane.

***holo*UnaG and *apo*UnaG.** To prepare *holo*UnaG (*i.e.*, the protein-encased bilirubin), a DMSO solution of bilirubin was added to an aqueous buffer solution containing *apo*UnaG (*i.e.*, the bilirubin-free protein) under conditions where the total amount of DMSO never

exceeded 5% (v/v). The solution thus obtained with a 2:1 bilirubin-to-protein ratio was incubated for 20 min with gentle stirring. *apo*UnaG fractions were likewise incubated with the same amount of DMSO lacking bilirubin to check for possible DMSO-induced denaturation of the UnaG protein. Samples were buffer changed in PD-10 desalting columns (GE Healthcare) to 50 mM PBS, 5 or 50 mM CAPS buffer or 20 mM citrate buffer. These buffer solutions were either D_2O- or H_2O-based, depending on the desired experiment.

The following procedure was used to verify that *holo*UnaG was correctly folded. Knowing that bilirubin and *apo*UnaG bind in a 1:1 ratio, we estimated the expected concentration of *holo*UnaG that would result from the admixture of known amounts of bilirubin and *apo*UnaG. Using the published value for the molar extinction coefficient of *holo*UnaG,[28] we then measured the concentration of *holo*UnaG isolated after a buffer change of our bilirubin-*apo*UnaG mixture on a PD-10 column. The data obtained indicate a 90% conversion of *apo*UnaG to *holo*UnaG. This number is well within the expected losses on a PD-10 column. This extent to which *holo*UnaG was recovered after the PD-10 column was also confirmed by comparing the relative intensities of *holo*UnaG fluorescence before and after running a PD-10 column. These data, along with the fact that our absorption and emission spectra of *holo*UnaG match those that have been published[28] indicate that our *holo*UnaG was correctly folded.

Instrumentation and Methods. Time-resolved $O_2(a^1\Delta_g)$ phosphorescence measurements were performed upon fs pulsed-laser excitation of a photosensitizer using an approach and instrumentation that has previously been described.[37, 38] Briefly, for the present study, the sensitizer $AlPcS_4$ was irradiated at 680 nm (1 kHz repetition rate, < 1.3 mW/cm^2 average power), and the 1275 nm $O_2(a^1\Delta_g)$ phosphorescence signal monitored using a cooled near-IR PMT operated in a photon counting mode. These experiments were performed using 1 cm

path length cuvettes under conditions where the sample absorbance at the irradiation wavelength did not exceed ~ 0.1. Data were obtained over an elapsed period of sample irradiation that did not exceed 30 s.

The procedure used in the kinetic competition studies to determine the reaction rate constant of *holo*UnaG with $O_2(a^1\Delta_g)$ has likewise been described previously.[39] The excitation source in these experiments was the attenuated output of a 150 W Xe lamp that had been passed through both a water filter and a 610 nm cut-on long pass filter. At these latter wavelengths, the sensitizer $AlPcS_4$ is the only light-absorbing molecule in the system. The solutions were stirred and the entire sample volume fully irradiated throughout these experiments. This approach was also used in the study to examine the response of *holo*UnaG to $O_2(a^1\Delta_g)$.

Steady-state absorption spectra were recorded either on a Shimadzu model UV3600 UV-VIS-NIR spectrometer or a Hewlett Packard diode array spectrometer (HP8453), and fluorescence spectra were recorded using a Fluoromax P spectrometer (Horiba Jobin Yvon). Circular dichroism (CD) data were collected using a JASCO-810 CD spectrometer equipped with a Peltier temperature-controlled cuvette holder in 1 mm path length cuvettes, and the average of at least 5 independent scans was used for a given spectrum.

Illustrations and computer-based analyses of the UnaG protein were performed with the UCSF Chimera package. Chimera is developed by the Resource for Biocomputing, Visualization, and Informatics at the University of California, San Francisco.[40]

RESULTS AND DISCUSSION

1. Absorption, fluorescence and CD spectra of bilirubin, *apo*UnaG and *holo*UnaG

Absorption and fluorescence spectra of free, solvated bilirubin and of bilirubin encased by UnaG (*i.e.*, *holo*UnaG) are shown in Figure 2. Also shown is the absorption

spectrum of the UnaG protein that lacks bilirubin (*i.e.*, *apo*UnaG). The data recorded were independent of whether a PBS (20 mM, pH 7.4) or a CAPS buffer was used (5 mM or 50 mM, pH 10.3). Identical data were likewise recorded when these buffers were prepared with D_2O instead of H_2O (pD 7.8 and 10.7, respectively).

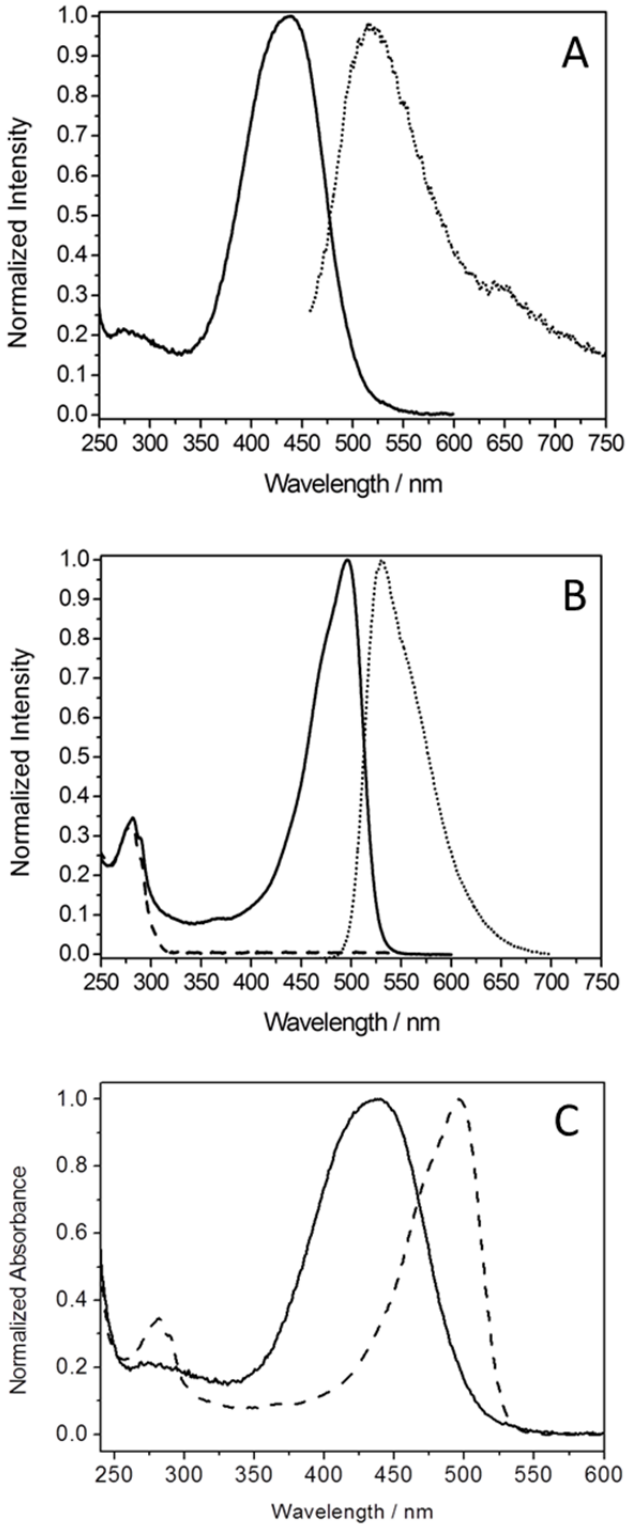

Figure 2. Absorption (solid lines) and emission (dotted lines) spectra, normalized to yield the same intensity at the band maximum, for bilirubin (panel A) and *holo*UnaG (panel B). Also shown in panel B is the absorption spectrum of *apo*UnaG (dashed line). These fluorescence spectra were recorded upon irradiation into the bilirubin absorption band at $\lambda = 440$ nm (free bilirubin) and $\lambda = 495$ nm (*holo*UnaG). The

bilirubin and *holo*UnaG absorption spectra shown in panels A and B are plotted together in panel C to better illustrate the differences between the two (bilirubin = solid line; *holo*UnaG = dashed line).

The effect of the encapsulating protein is perhaps most clearly seen by the pronounced shift in the maximum of the bilirubin absorption band from ~ 440 to 495 nm. (Note that the absorption band with a maximum at ~ 280 nm, assigned to tryptophan and tyrosine residues in the protein, does not shift upon binding bilirubin.) These changes suggest that different environment-dependent conformational/configurational isomers of bilirubin may be involved in the transition.[29, 30] In contrast, there is not a particularly large protein dependent change in the bilirubin fluorescence spectrum (Figure 2).

The quantum yield of bilirubin fluorescence has been reported to increase from ~ 10^{-3} for the free solvated molecule to ~ 0.5 for the UnaG-encased molecule.[28, 34] The latter likely reflects the geometric constraints of the protein enclosure that inhibit conformational changes in the chromophore which facilitate nonradiative deactivation channels.

Fluorescence spectra recorded upon irradiation of both *apo*UnaG and *holo*UnaG at 290 nm, where the principal absorbing chromophores are tryptophan and tyrosine residues in the protein, show a small bilirubin-dependent red shift (~ 5 nm) in the emission band maximum suggesting only a slight bilirubin-dependent perturbation of the electronic state energies of these amino acid residues (Figure 3). This conclusion is consistent with the observed lack of a bilirubin-dependent change in the absorption band centered at ~ 280 nm (*vide supra*, Figure 2). In contrast, the intensity of the emission assigned to these amino acid residues decreases appreciably upon the incorporation of bilirubin into the protein (Figure 3). This observation may reflect energy transfer from the excited states of the amino acid residues to bilirubin. This interpretation is reasonable given that there are four tyrosine residues that are less than 3.5 Å away from bilirubin and one tryptophan residue that is ~ 7 Å away from

bilirubin. Unfortunately, experiments to test this hypothesis are confounded by the fact that it is difficult to irradiate at ~ 280-300 nm (*i.e.*, populate the protein excited state) without concurrently populating the bilirubin excited state and thereby directly producing bilirubin fluorescence (*i.e.*, bilirubin also has a small absorption at ~ 280-300 nm). On the other hand, data collected from bilirubin bleaching experiments are consistent with this energy transfer hypothesis (*vide infra*).

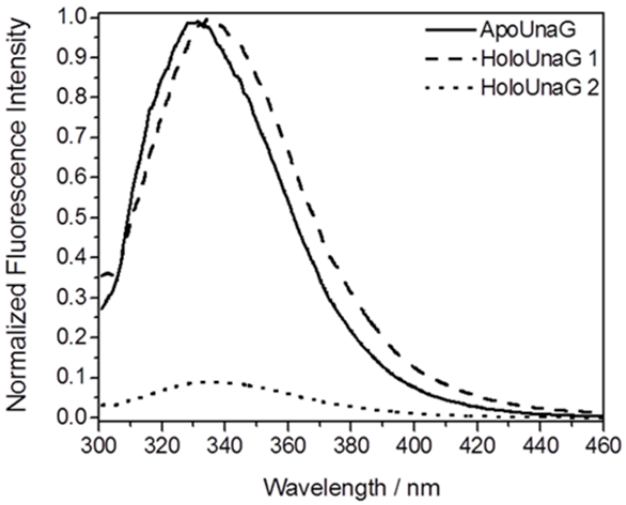

Figure 3. Fluorescence spectra recorded upon irradiating *apo*UnaG and *holo*UnaG at 290 nm where the principal absorbing chromophores are tryptophan and tyrosine residues in the protein. The *apo*UnaG spectrum is shown as a solid line. The *holo*UnaG data are presented in two different ways: (1) scaled such that the intensity of the band maximum is the same as that for the *apo*UnaG data to best show the spectral shift (dashed line) and (2) unscaled to show the intensity difference between the *holo* and *apo* samples (dotted line).

CD spectroscopy provides information about a protein's secondary structure by probing the difference in absorbance of left- and right-circularly polarized light. This difference depends on the alignment of the asymmetric carbons that constitute the protein backbone. A CD spectrum thus allows one to comment on the relative contribution of α-

helices, β-sheets and random coils to the overall protein structure.[41] The CD spectra of *apo*UnaG and *holo*UnaG are shown in Figure 4.

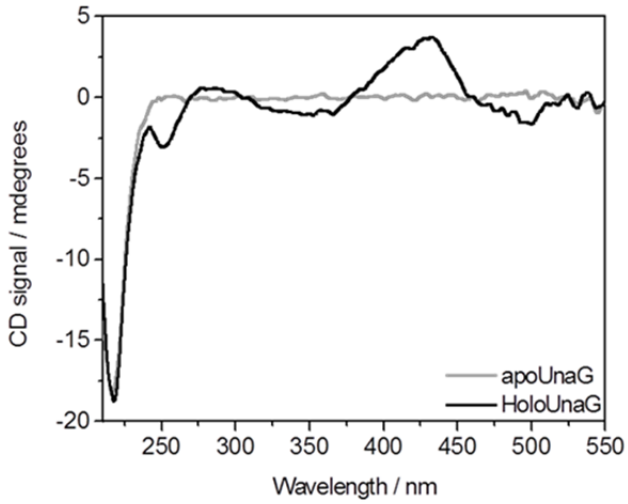

Figure 4. CD spectra for *holo*UnaG (black line) and *apo*UnaG (grey line).

The CD spectra over the range ~ 220-270 nm for both *apo*UnaG and *holo*UnaG are consistent with structures that contain mostly β-sheets, and this is in accord with the crystal structure available for *holo*UnaG (Figure 1).[28] In the *holo*UnaG spectrum, the combination of the positive couplet at 250(-)/285(+) nm and the negative couplet at 425(+)/480(-) nm is consistent with the binding of the chiral P-helical isomer of bilirubin in the protein. This characteristic signal has been observed and assigned for HSA- and BSA-bound bilirubin,[42, 43] and contrasts markedly with data recorded from bilirubin in an isotropic solvent. For the latter, a racemic mixture of the M- and P-helical conformers of bilirubin give rise to the absence of a CD signal.[44]

A denaturation study was performed by monitoring the change in the CD signal at 220 nm as a function of temperature. The data showed that *apo*UnaG denatures at a much lower temperature (51 °C) than *holo*UnaG (66 °C) indicating that the binding of bilirubin increases the stability of the protein.

2. Bilirubin and *holo*UnaG do not sensitize the production of $O_2(a^1\Delta_g)$

To fully characterize the behavior of bilirubin and *holo*UnaG with respect to processes that involve $O_2(a^1\Delta_g)$, it is essential to ascertain whether these systems themselves sensitize the production of $O_2(a^1\Delta_g)$ upon irradiation. To this end, we irradiated both bilirubin and, independently, *holo*UnaG at 420 nm using a pulsed fs laser. In each case, samples were prepared to have an absorbance of 0.1 over a 1 cm path length at this wavelength. We then looked for the characteristic 1275 nm phosphorescence of $O_2(a^1\Delta_g)$ in time-resolved photon-counting experiments. These studies were performed in D_2O-based buffers to capitalize on the H_2O/D_2O solvent isotope effect on the lifetime of $O_2(a^1\Delta_g)$ that, in turn, increases the quantum efficiency of $O_2(a^1\Delta_g)$ phosphorescence in D_2O.[26, 45]

In both cases, we were not able to detect a $O_2(a^1\Delta_g)$ phosphorescence signal. Given the detection parameters of our system, we can thus state that the photosensitized quantum yield of $O_2(a^1\Delta_g)$ production for both bilirubin and *holo*UnaG does not exceed 0.001. This is a desired attribute of a probe for $O_2(a^1\Delta_g)$.[25, 46]

3. Effects of $O_2(a^1\Delta_g)$ on *apo*UnaG and *holo*UnaG

To examine the effects of $O_2(a^1\Delta_g)$ on *apo*UnaG and *holo*UnaG, we generated $O_2(a^1\Delta_g)$ using a photosensitizer that was added to the buffer solution containing the proteins. The water-soluble molecule $AlPcS_4$ was used for this purpose. $AlPcS_4$ was chosen principally because it has an absorption band maximum at 680 nm, and this allows us to selectively irradiate this sensitizer without putting any light into *apo*UnaG or *holo*UnaG (Figure 2). $AlPcS_4$ sensitizes the production of $O_2(a^1\Delta_g)$ with a quantum yield of 0.22 ± 0.03.[47] Because the $AlPcS_4$ concentration used in our experiments was ~ 1 μM, the steady-state concentration

of $O_2(a^1\Delta_g)$ produced upon irradiation of $AlPcS_4$ with the filtered output of the *cw* Xe lamp was thus always very small.

Proteins can interact with phthalocyanines and thereby perturb their photophysical properties.[48] However, under our experimental conditions, we did not observe appreciable changes in the absorption and emission spectra of bilirubin, *apo*UnaG, *holo*UnaG and $AlPcS_4$ upon admixture of these respective molecules. Thus, we assume that $AlPcS_4$ and the proteins are homogenously distributed in our buffered solutions and that our data do not show the effects of aggregation and/or complexation.

Absorption and emission spectra of both *apo*UnaG and *holo*UnaG were recorded as a function of the elapsed irradiation time of co-dissolved $AlPcS_4$ (Figure 5). The data in Figures 5A and 5B show an appreciable and correlated decrease in the bilirubin absorbance and fluorescence intensity as a function of prolonged exposure of *holo*UnaG to $O_2(a^1\Delta_g)$. The clear absence of a spectral shift and an isosbestic point in the absorption spectra strongly suggests that these data reflect the expected oxidation of the encapsulated bilirubin rather than the release of bilirubin to the solvent due to the oxidation of amino acid residues in the protein that influence bilirubin binding (see Figure 2C for reference). Data recorded from *apo*UnaG (Figure 5C) demonstrate that, in the absence of encapsulated bilirubin, the tryptophan and tyrosine residues in the protein are indeed susceptible to oxidation by $O_2(a^1\Delta_g)$. As noted from a plethora of other proteins, this is an expected observation.[49, 50] However, the data in Figure 5D suggest that the presence of bilirubin in the protein serves to inhibit the oxidation of the tryptophan and tyrosine residues, perhaps through its role as a self-sacrificing scavenger of $O_2(a^1\Delta_g)$. In support of this latter suggestion, we note that $O_2(a^1\Delta_g)$ produced outside of the protein (*i.e.*, via $AlPcS_4$ sensitization) will encounter bilirubin principally upon diffusion through a discrete "entry port" (see Figure 2). Furthermore, relative to this entry

port, the pertinent tryptophan and tyrosine residues are behind the bilirubin molecule. Thus, $O_2(a^1\Delta_g)$ will encounter bilirubin before encountering these reactive amino acid residues.

In support of our suggestion that bilirubin can quench, via energy transfer, the fluorescence of the tryptophan and tyrosine residues in UnaG upon irradiation of these residues at ~ 290 nm (*vide supra*), we observe that a $O_2(a^1\Delta_g)$-induced bleaching of bilirubin (Figure 5 A and B) correlates with a systematic increase in the fluorescence intensity assigned to the tryptophan and tyrosine residues in the protein (Figure 5 D).

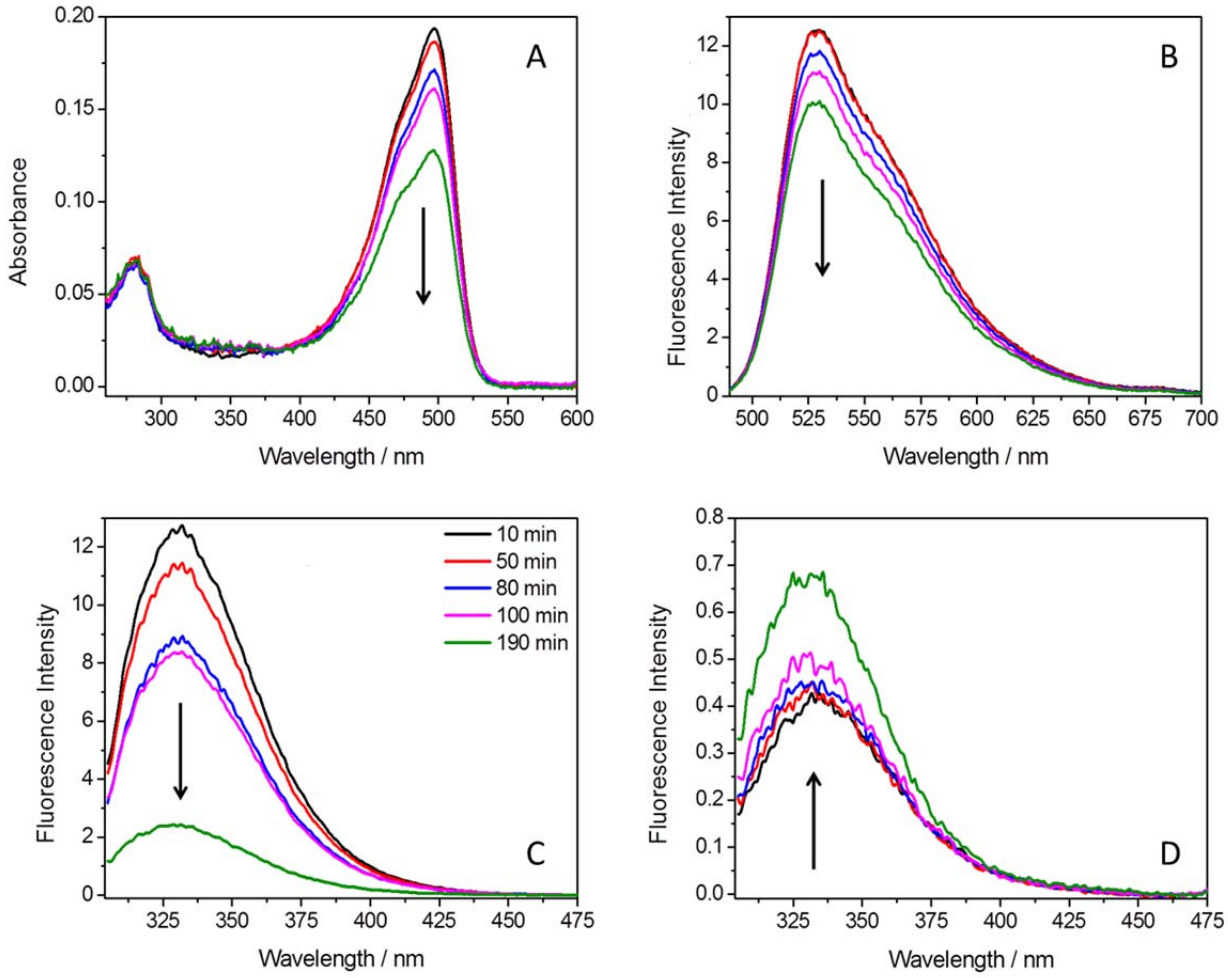

Figure 5. Absorption (panel A) and fluorescence (panel B) spectra of *holo*UnaG recorded as a function of the elapsed irradiation time of co-dissolved $AlPcS_4$. Corresponding $AlPcS_4$-irradiation-dependent fluorescence spectra recorded from solutions of

*apo*UnaG (panel C) and *holo*UnaG (panel D) obtained using a different wavelength to excite fluorescence (290 nm) to specifically focus on emission from the protein at ~ 320-375 nm. Note the differences in the relative scaling factors used on the ordinates of the fluorescence spectra in panels C and D.

4. Effects of superoxide on *holo*UnaG

In photosensitized oxidations in biologically pertinent systems, certainly those containing proteins, photoinitiated electron transfer to produce the superoxide ion often kinetically competes with the sensitized production of $O_2(a^1\Delta_g)$.[13, 51] Indeed, the superoxide ion is a relevant and ubiquitous ROS, and it is known to result in the oxidative degradation of both bilirubin and proteins.[52-55] With this in mind, it is incumbent upon us to ascertain how *holo*UnaG responds to the presence of the superoxide ion.

When assessing the effects of the superoxide ion, it is common practice to add an aqueous solution of potassium superoxide as a reagent to the system of interest. However, to minimize the effects of superoxide protonation and disproportionation that would decrease the concentration of superoxide in an aqueous reagent,[56] we opted to directly add potassium superoxide as a powder to our aqueous solution of *holo*UnaG (PBS buffered solution at pH 7.4). Under our conditions, based on the amount of added powder, the maximum concentration of superoxide thus achieved was ~ 100 mM, which is an amount that far exceeds the steady-state concentration of $O_2(a^1\Delta_g)$ produced in the preceding experiments (*vide supra*).

Absorption and fluorescence spectra of *holo*UnaG, recorded as a function of increasing amounts of added potassium superoxide, are shown in Figure 6. The absorption spectra shown in Figure 6A provide a distinct contrast to what is shown in Figure 5A for the reaction of *holo*UnaG with $O_2(a^1\Delta_g)$. Specifically, for the reaction with superoxide, distinct

isosbestic points are observed that implicate the superoxide-mediated production of a compound that has a blue-shifted spectrum different from that of *holo*UnaG. A logical candidate for this compound is bilirubin itself that has been released from its binding site in the protein. The corresponding superoxide-concentration-dependent fluorescence spectra shown in Figure 6B are consistent with this interpretation; a pronounced spectral shift in the fluorescence spectrum is not observed as expected from the data in Figure 2, but the decrease in intensity is consistent with the smaller quantum yield of fluorescence for free bilirubin solvated in the aqueous medium.

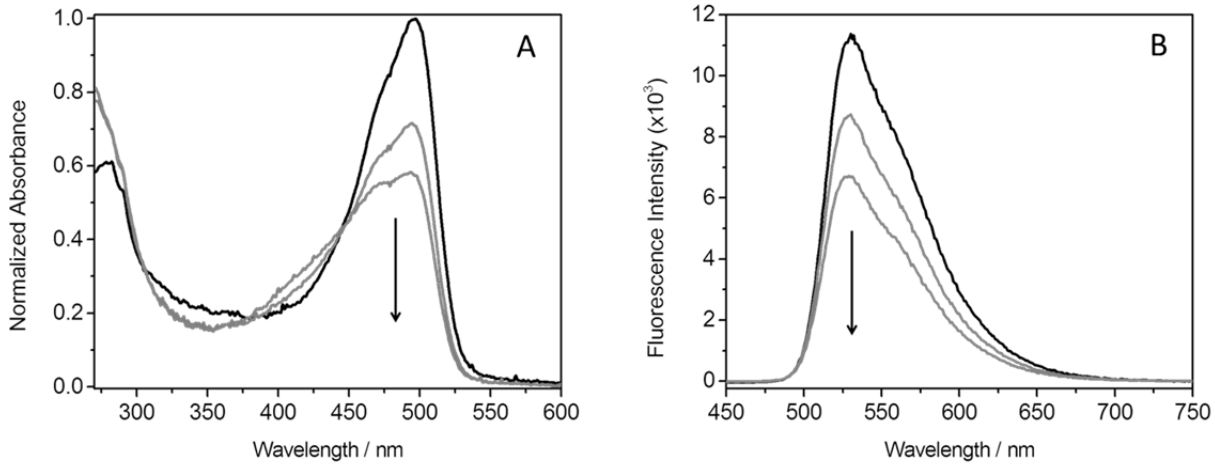

Figure 6. Absorption (A) and fluorescence (B) spectra recorded as a function of increasing amounts of powdered potassium superoxide added to an aqueous solution of *holo*UnaG (PBS buffer at pH 7.4).

The data in Figure 6, and our associated interpretation, are certainly reasonable given the known superoxide-mediated radical processes that can result in protein oxidation.[53-55] Most importantly, and again within the context of developing a system that uniquely responds to $O_2(a^1\Delta_g)$, the rate constants for the reaction of superoxide and hydroperoxyl radicals with amino acids are quite small ($< 10^2$ s^{-1} M^{-1}),[57] and are certainly smaller than the pertinent rate constants for reaction with $O_2(a^1\Delta_g)$ (*vide infra*). This information, coupled with the relative

concentrations of $O_2(a^1\Delta_g)$ and superoxide that yield the data shown in Figures 5 and 6, indicates that *holo*UnaG is indeed a system that preferentially responds to $O_2(a^1\Delta_g)$. This conclusion is consistent with data obtained for the analogous protein-encapsulated biliverdin system; it too preferentially responds to $O_2(a^1\Delta_g)$ and not the superoxide ion.[35]

4. Quantifying rate constants for interaction with $O_2(a^1\Delta_g)$

When considering events that result in the removal of $O_2(a^1\Delta_g)$ from a given system, it is important to recognize that the chemical reactions of $O_2(a^1\Delta_g)$ kinetically compete with processes wherein $O_2(a^1\Delta_g)$ is deactivated to $O_2(X^3\Sigma_g^-)$.[26] This deactivation could be the result of interactions with (1) a solute acting not just as a chemical "reactant" but also as a so-called "quencher" and (2) solvent molecules. The overall rate constant for $O_2(a^1\Delta_g)$ removal, k_Δ, can thus be expressed as a sum of bimolecular terms as shown in eq 1,

$$k_\Delta = k_{nr}[S] + k_r[S] + k_q[Q] + k_{rxn}[R] \qquad (1)$$

where R and Q represent the chemical reactant and quencher, respectively, and S represents the solvent. The solvent-dependent deactivation terms are further subdivided into a nonradiative process, k_{nr}, and a radiative process, k_r. The latter corresponds to the $O_2(a^1\Delta_g) \rightarrow O_2(X^3\Sigma_g^-)$ phosphorescence at ~ 1275 nm. The reciprocal of the first-order rate constant k_Δ defines the lifetime of $O_2(a^1\Delta_g)$, τ_Δ.

For bilirubin dissolved in an aqueous buffer, $R = Q$ and the kinetic competition between the channels of non-reactive and reactive $O_2(a^1\Delta_g)$ removal depend solely on the magnitudes of the rate constants k_q and k_{rxn}, respectively. For bilirubin encapsulated in the

UnaG protein, one must also consider corresponding values of k_q and k_{rxn} for the interaction between the protein and $O_2(a^1\Delta_g)$ when defining k_Δ.

The overall bimolecular rate constants for bilirubin-, *apo*UnaG, and *holo*UnaG-mediated $O_2(a^1\Delta_g)$ removal, k_{rem}, that represent the sums of these k_q and k_{rxn} terms are readily obtained from time-resolved $O_2(a^1\Delta_g)$ phosphorescence experiments in which values of k_Δ are determined as a function of the concentration of added bilirubin, *apo*UnaG, and *holo*UnaG.[13, 26] However, distinguishing between k_q and k_{rxn} for bilirubin in *holo*UnaG will require a separate experiment that quantifies the rate of the chemical reaction that results in the bleaching of bilirubin in the protein.[39] We address these issues, respectively, in the sections below.

4.1. Overall bilirubin-, apoUnaG-, and holoUnaG-mediated $O_2(a^1\Delta_g)$ removal

For these experiments, $O_2(a^1\Delta_g)$ was generated by the irradiation of $AlPcS_4$ co-dissolved in solutions of bilirubin and, independently, *apo*UnaG and *holo*UnaG. Time-resolved $O_2(a^1\Delta_g)$ phosphorescence traces were then recorded, and the resultant values of k_Δ plotted against the concentration of bilirubin, *apo*UnaG and *holo*UnaG used in a given experiment (Figure 7). To increase the accuracy of the k_{rem} value obtained, these experiments were performed using D_2O-based solutions to exploit the known H_2O/D_2O solvent isotope effect on k_{nr} and, thereby, minimize the effects of solvent-mediated $O_2(a^1\Delta_g)$ deactivation.[13, 26] Indeed, this is an important aspect of the study since the *holo*UnaG-dependent changes in the $O_2(a^1\Delta_g)$ kinetic signal were very subtle (see Figure 7). The fact that the absorption spectra of *holo*UnaG, in particular, are independent of whether a D_2O-based or H_2O-based buffer is used (*vide supra*) indicates that this change of solvent does not influence the binding of bilirubin by the protein. The values of k_{rem} thus obtained are shown in Table 1.

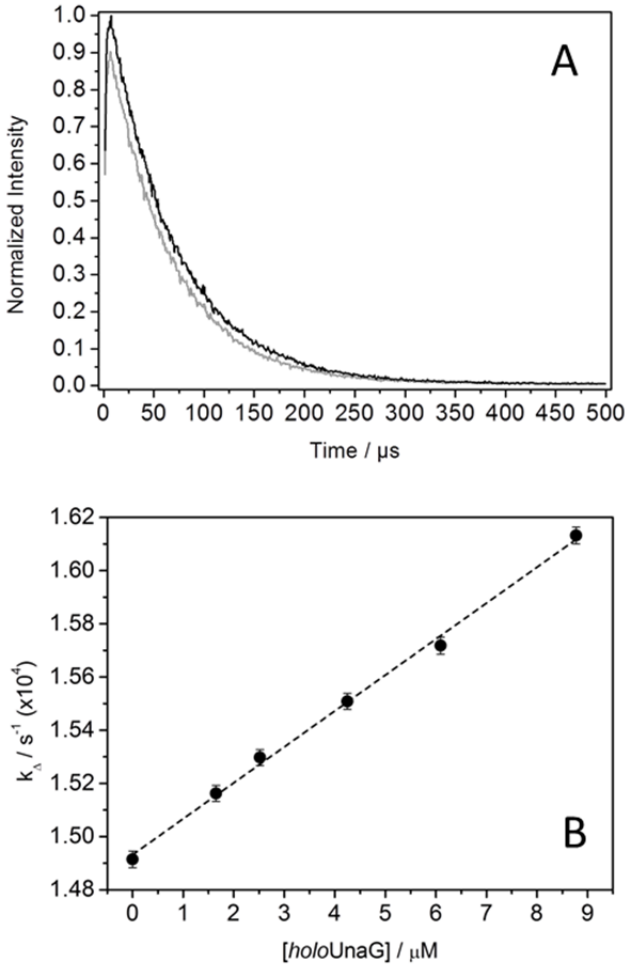

Figure 7. (A) Examples of the time-resolved 1275 nm $O_2(a^1\Delta_g)$ phosphorescence traces used to quantify the overall rate constant for $O_2(a^1\Delta_g)$ removal by *holo*UnaG. The trace shown in black was recorded in the absence of added *holo*UnaG, whereas the trace shown in grey was recorded at the highest concentration of *holo*UnaG used, 9 μM. (B) The corresponding plot of k_Δ against [*holo*UnaG] that yields the value of k_{rem} from the slope.

Table 1. Values of the overall rate constant for $O_2(a^1\Delta_g)$ removal, k_{rem}, mediated by bilirubin, *apo*UnaG and *holo*UnaG obtained from $O_2(a^1\Delta_g)$ phosphorescence experiments.

Compound	pD	k_{rem} (10^8 M^{-1} s^{-1})
Bilirubin	6.4	< 0.1
	7.8	4.3 ± 0.6
	10.7	12.0 ± 0.5
*holo*UnaG	7.8	1.4 ± 0.1
	10.7	1.9 ± 0.3
*apo*UnaG	7.8	1.5 ± 0.1
	10.7	2.7 ± 0.2

Our data show that the overall rate constant for $O_2(a^1\Delta_g)$ removal by free, solvated bilirubin increases appreciably as the solution become more alkaline. This observation is consistent with the results of experiments published in 1974,[58] although this 1974 publication has been criticized for a number of different reasons.[31] In any event, it is clear that the bilirubin anion/dianion is more effective at removing $O_2(a^1\Delta_g)$ than the neutral form of the molecule. This is reasonable since $O_2(a^1\Delta_g)$ is an electrophile and is known to react rapidly with electron rich and more easily oxidized species.[26, 59] Moreover, electron-rich and easily-oxidized species facilitate the formation of charge-transfer states upon interaction with $O_2(a^1\Delta_g)$, which promotes the nonradiative deactivation of $O_2(a^1\Delta_g)$ to $O_2(X^3\Sigma_g^-)$.[26, 60] With this interpretation in mind, the pD-dependent values of k_{rem} shown in Table 1 are consistent with revised p*K*a values of bilirubin that have recently been published.[61]

The data also clearly show that encapsulating bilirubin in the UnaG protein results in an appreciable decrease in the magnitude of k_{rem}. Given the absolute magnitude of the rate

constants involved (*i.e.*, ~ 10^8 – 10^9 M^{-1} s^{-1}), it is likely that this observation mostly reflects the fact that $O_2(a^1\Delta_g)$ must now diffuse through the encasing protein before it can encounter bilirubin (*vide supra*, Figure 1). This assessment is based on analogous $O_2(a^1\Delta_g)$ experiments performed in media with different viscosities using reactants that cover the range from diffusion- to preequilibrium-limited processes.[62] Although oxygen diffusion through proteins has been studied for many years,[63, 64] it is only recently that aspects of this problem pertinent to $O_2(a^1\Delta_g)$ have been investigated.[39, 51, 65-68] In any event, this diffusion-dependent interpretation is reasonable given what is known about the structure of *holo*UnaG and what has been observed for somewhat related protein-encapsulated chromophores.[39, 65, 67] Nevertheless, one must also consider protein-dependent changes in k_q and k_{rxn}, both of which combine to define k_{rem}. We have independently shown that a protein environment can significantly alter these rate constants,[39] a point which is addressed in the next section in an experiment to quantify k_{rxn} for *holo*UnaG.

The absence of an appreciable pD-dependent change in k_{rem} for *holo*UnaG, in comparison to that observed for bilirubin, could reflect a protein-dependent change in the pK_a of bound bilirubin (*i.e.*, the protein-bound bilirubin is less apt to lose protons to form the anion/dianion[61]).

The values of k_{rem} obtained for *apo*UnaG are very similar to those obtained for *holo*UnaG. However, care must be exercised in assuming that the *apo*UnaG data provide an appropriate control that allows us to distinguish between the effects of bilirubin and the surrounding protein on $O_2(a^1\Delta_g)$ removal in *holo*UnaG. Specifically, in the absence of bilirubin, UnaG presents amino acids that can more readily interact with $O_2(a^1\Delta_g)$ and thereby give a much larger value of k_{rem}.[28] Thus, the k_{rem} value for *apo*UnaG does not adequately represent the protein-dependent component of k_{rem} in *holo*UnaG. In short, when considered alone, the *apo*UnaG and *holo*UnaG data in Table 1 may lead to the potentially incorrect

conclusion that, in *holo*UnaG, $O_2(a^1\Delta_g)$ removal is dominated by interactions with the protein and not bilirubin. In the least, the data shown in Figures 5A and 5B certainly indicate that, when incorporated in the UnaG protein, bilirubin can still react with $O_2(a^1\Delta_g)$ at an appreciable rate.

For *apo*UnaG, the slight increase in k_{rem} with the increase in pD may reflect the relative instability of this protein when bilirubin is not bound (*vide supra*). In short, an alkaline-induced denaturation of the protein[69] would expose amino acids that, in turn, could result in an increase in k_{rem}. Alternatively, and as discussed above with respect to the deprotonation of free bilirubin, an increase in pD could likewise result in the deprotonation of amino acid residues in the protein. The resultant electron-rich anion (*e.g.*, the tyrosine phenolate) would be a more efficient quencher of $O_2(a^1\Delta_g)$.

To complement the *apo*UnaG and *holo*UnaG data shown in Table 1, we used this same approach of monitoring $O_2(a^1\Delta_g)$ phosphorescence to quantify k_{rem} for a variety of other commonly-found proteins. These data are shown in Table 2. To our knowledge, only a value for HSA has been previously reported, $(5 \pm 3) \times 10^8$ s^{-1} M^{-1},[48] and our value of $(2.6 \pm 0.5) \times 10^8$ s^{-1} M^{-1} compares well with this number.

Table 2. Values of the overall rate constant for $O_2(a^1\Delta_g)$ removal, k_{rem}, mediated by selected proteins obtained from $O_2(a^1\Delta_g)$ phosphorescence experiments.[a]

Compound	k_{rem} (10^8 M^{-1} s^{-1})
BSA	0.40 ± 0.06
BSA-fatty acid free	0.24 ± 0.04
HSA	2.6 ± 0.5
HSA-fatty acid free	1.9 ± 0.3
RSA	4.1 ± 0.2

(a) Experiments were performed in D_2O-based PBS (pD 7.8) using perinaphthenone sulfonic acid as the $O_2(a^1\Delta_g)$ sensitizer.

4.2. Rate constants for the reaction between holoUnaG and $O_2(a^1\Delta_g)$

If we assume that the changes in the spectra of protein-encased bilirubin shown in Figures 5A and 5B are a direct result of the $AlPcS_4$-sensitized production of $O_2(a^1\Delta_g)$ in the medium surrounding *holo*UnaG (*i.e.*, secondary $O_2(a^1\Delta_g)$-initiated radical reactions that derive from protein oxidation play a minor role over the time scale of our experiments), then we can use these spectral changes to quantify k_{rxn} for the reaction between $O_2(a^1\Delta_g)$ and the protein-encased bilirubin.

Our approach to quantify k_{rxn} has been previously described in detail.[39] Briefly, for the present study, we (1) generated a population of $O_2(a^1\Delta_g)$ in the surrounding solvent using co-dissolved $AlPcS_4$ as a photosensitizer, (2) monitored the extent to which the ~ 525 nm fluorescence from *holo*UnaG is "bleached" in the presence of $O_2(a^1\Delta_g)$, and (3) compared this change in *holo*UnaG fluorescence intensity to the corresponding change in fluorescence intensity of a standard molecule that kinetically competes with the bilirubin-containing

protein for the available $O_2(a^1\Delta_g)$. Through the use of eq 2, we then obtained the desired rate constant, k_{rxn}, for the reaction of $O_2(a^1\Delta_g)$ with bilirubin in *holo*UnaG.

$$\frac{k_{rxn}}{k_{rxn}^{standard}} = \frac{\log\left(\frac{I_t^{holoUnaG}}{I_0^{holoUnaG}}\right)}{\log\left(\frac{I_t^{standard}}{I_0^{standard}}\right)} \qquad (2)$$

In eq 2, $k_{rxn}^{standard}$ is the known rate constant for the reaction of $O_2(a^1\Delta_g)$ with the standard molecule, I_0 is the fluorescence intensity of the given compound at time = 0 (*i.e.*, before the production of $O_2(a^1\Delta_g)$), and I_t is the fluorescence intensity after some time t of elapsed irradiation of the sensitizer.

The standard used for this kinetic competition was 9,10-anthracenediyl-bis(methylene)dimalonic acid (ADA).[39, 70] ADA has a distinct fluorescence spectrum that is likewise "bleached" when ADA reacts with $O_2(a^1\Delta_g)$ to form an endoperoxide (Figure 8). The rate constant for the reaction of ADA with $O_2(a^1\Delta_g)$ is $(5.5 \pm 0.5) \times 10^7$ $s^{-1}M^{-1}$.[39]

It is also important to note that we did not observe changes in the absorption and emission spectra of *holo*UnaG, ADA and $AlPcS_4$ upon admixture of these respective molecules. Therefore, the data thus obtained do not show the effects of aggregation and/or complexation of these solutes in our buffered solutions.

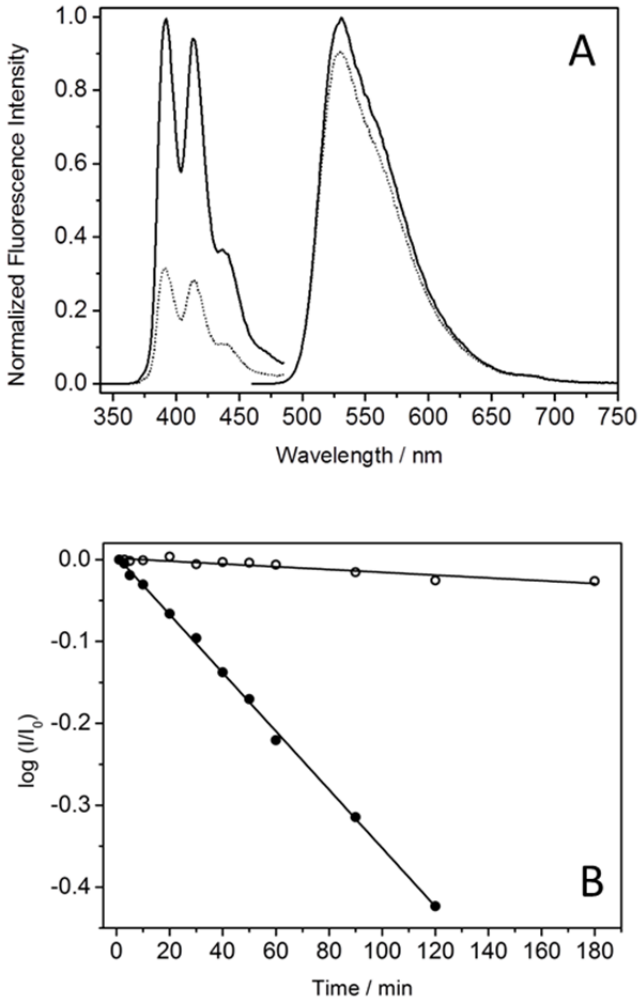

Figure 8. (A) Examples of the pertinent fluorescence spectra used in the experiment where ADA kinetically competes with *holo*UnaG for the $O_2(a^1\Delta_g)$ produced upon irradiation of $AlPcS_4$. The solid lines show the spectra of ADA (left) and *holo*UnaG (right) prior to the production of $O_2(a^1\Delta_g)$, and the dashed lines show the corresponding spectra after irradiating $AlPcS_4$ for 180 min at $\lambda > 610$ nm with the output of a filtered Xe lamp. (B) Plots of the normalized fluorescence intensity obtained from *holo*UnaG (open circles) and ADA (filled circles) used with eq 2 to obtain k_{rxn} for *holo*UnaG. Experiments were performed in H_2O-based solutions at pH 7.4.

Using eq 2 and the data shown in Figure 8, we obtain a value of k_{rxn} for *holo*UnaG of $(2.4 \pm 0.4) \times 10^6$ M^{-1} s^{-1}. Comparing this value to the corresponding value of k_{rem} shown in Table 1 yields $k_{rxn}/k_{rem} = 0.017 \pm 0.004$. This ratio for protein-encased bilirubin is

approximately ten times smaller than the corresponding ratio reported for bilirubin dissolved in chloroform; 0.16.[31] Thus, not only do the absolute magnitudes of k_{rem} and k_{rxn} decrease upon protein encapsulation, but the fraction of the total bilirubin-induced process of $O_2(a^1\Delta_g)$ removal that occurs via a chemical reaction also decreases appreciably.

5. *holo*UnaG as a $O_2(a^1\Delta_g)$ probe

It remains now to discuss the results presented above with respect to the use of *holo*UnaG as a $O_2(a^1\Delta_g)$ probe or as a system that can selectively perturb a local population of $O_2(a^1\Delta_g)$ that might be produced in a cell, for example. As stated at the outset, the intent is to establish a quantitative framework by which other protein-encapsulated probes for $O_2(a^1\Delta_g)$ can also be evaluated.

The first, and arguably most important, limitation of *holo*UnaG is that the rate constant for the overall removal of $O_2(a^1\Delta_g)$, $1.4 \pm 0.1 \times 10^8$ M^{-1} s^{-1}, is not appreciably larger than the rate constants for $O_2(a^1\Delta_g)$ removal by typical proteins (*e.g.*, data in Table 2). Thus, when inserted into a protein-rich environment at a presumably low concentration, *holo*UnaG would not stand out as a system that perturbs the local $O_2(a^1\Delta_g)$ population. However, if we recognize that this comparatively small k_{rem} value of $1.4 \pm 0.1 \times 10^8$ M^{-1} s^{-1} principally reflects the fact that the protein enclosure inhibits $O_2(a^1\Delta_g)$ diffusional access to the reasonably effective quencher bilirubin, for which values of k_{rem} as large as $\sim 3 \times 10^9$ M^{-1} s^{-1} have been reported in a bulk solvent,[31] then there is sufficient justification to be optimistic. Specifically, a protein mutation that does not change the binding of bilirubin but that facilitates better diffusional access to oxygen should make a difference in this regard.

For the development of a fluorescent probe that responds to $O_2(a^1\Delta_g)$, it would be desirable to have a k_{rxn}/k_{rem} ratio that is larger than the value of ~ 0.02 measured in the present study. With respect to this point, there is again sufficient justification to be optimistic. First,

subtle changes in the protein environment immediately surrounding a $O_2(a^1\Delta_g)$ substrate can perturb the charge distribution of the substrate. In turn, this can result in an appreciable increase in the rate constant for reaction with $O_2(a^1\Delta_g)$.[39] Thus, we should consider a judicious protein mutation that likewise does not change the binding constant for bilirubin but that puts amino acid residues in positions that render selected double bonds in bilirubin more electron-rich and thus more reactive to $O_2(a^1\Delta_g)$. Second, given the structural and $O_2(a^1\Delta_g)$-related kinetic similarities between bilirubin and biliverdin,[27] the report that protein-encased biliverdin has already been successfully used as an intracellular fluorescent probe for $O_2(a^1\Delta_g)$ certainly establishes important precedence.

Admittedly, for both bilirubin and biliverdin, the fact that the response to $O_2(a^1\Delta_g)$ is based on a reaction-dependent decrease in fluorescence intensity (*e.g.*, Figure 5 B) is not ideal. Rather, it is arguably more desirable to have a probe whose fluorescence intensity increases from zero (*i.e.*, dark) upon reaction with $O_2(a^1\Delta_g)$.[19, 25] At present, the limiting factor with respect to this latter point is the incorporation of the appropriate fluorophore in a genetically-encodable protein. Carrying this latter point further, despite a large binding constant for bilirubin in the protein, the ambient bilirubin concentration in selected mammalian cells, where bilirubin is endogenously produced, may be sufficiently high under certain circumstances to mitigate the effect of this particular probe molecule. Thus, in selected cases, one might indeed want to consider the use of a probe molecule not normally found in a cell. "Problems" such as this continue to provide a general challenge in the field, indicating that perfect solutions still do not exist.[71] Nevertheless, these issues do not invalidate the importance of the kinetic conclusions drawn from the present bilirubin model system.

CONCLUSIONS

Experiments have been performed to characterize and quantify interactions between $O_2(a^1\Delta_g)$ and bilirubin encased in a protein. The specific system studied here, a bilirubin-binding protein isolated from a freshwater Japanese eel, arguably does not satisfy the ideal kinetic criteria for a probe that can be used in mechanistic studies of $O_2(a^1\Delta_g)$ performed in cells. Nevertheless, this system provides much-needed quantitative insight into parameters that must be considered in the development of an acceptable protein-encased $O_2(a^1\Delta_g)$ probe.

Acknowledgements

This work was supported by grants from the Danish National Research Foundation and the EU Marie Curie Training Program (TopBio PITN-GA-2010-264362). The authors thank Anette Kjems for assistance with the expression and purification of UnaG.

References

1 B. Halliwell and J. M. C. Gutteridge, *Free Radicals in Biology and Medicine*, Oxford University Press, Oxford, 1999.

2 J. T. Hancock, *Cell Signalling*, Oxford University Press, Oxford, 2005.

3 C. C. Winterbourn, Reconciling the chemistry and biology of reactive oxygen species, *Nature Chemical Biology*, 2008, **4**, 278-286.

4 M. L. Circu and T. Y. Aw, Reactive Oxygen Species, Cellular Redox Systems, and Apoptosis, *Free Rad. Biol. Med.*, 2010, **48**, 749-762.

5 B. C. Dickinson and C. J. Chang, Chemistry and Biology of Reactive Oxygen Species in Signaling or Stress Responses, *Nature Chemical Biology*, 2011, **7**, 504-511.

6 K. Setsukinai, Y. Urano, K. Kakinuma, H. J. Majima and T. Nagano, Development of Novel Fluorescence Probes that can Reliably Detect Reactive Oxygen Species and Distinguish Specific Species., *J. Biol. Chem.*, 2003, **278**, 3170-3175.

7 A. Gomes, E. Fernandes and J. L. F. C. Lima, Fluorescence Probes used for Detection of Reactive Oxygen Species, *J. Biochem. Biophys. Methods*, 2005, **65**, 45-80.

8 P. Wardman, Fluorescent and Luminescent Probes for Measurement of Oxidative and Nitrosative Species in Cells and Tissues: Progress, Pitfalls, and Prospects., *Free Rad. Biol. Med.*, 2007, **43**, 995-1022.

9 J. Chan, S. C. Dodani and C. J. Chang, Reaction-Based Small-Molecule Fluorescent Probes for Chemoselective Bioimaging, *Nature Chemistry*, 2012, **4**, 973-984.

10 X. Li, X. Gao, W. Shi and H. Ma, Design Strategies for Water-Soluble Small Molecular Chromogenic and Fluorogenic Probes, *Chem. Rev.*, 2014, **114**, 590-659.

11 B. N. G. Giepmans, S. R. Adams, M. H. Ellisman and R. Y. Tsien, The Fluorescent Toolbox for Assessing Protein Location and Function, *Science*, 2006, **312**, 217-224.

12 K. A. Lukyanov and V. V. Belousov, Genetically Encoded Fluorescent Redox Sensors, *Biochim. Biophys. Acta*, 2014, **1840**, 745-756.

13 P. R. Ogilby, Singlet Oxygen: There is Indeed Something New Under the Sun., *Chem. Soc. Rev.*, 2010, **39**, 3181-3209.

14 R. W. Redmond and I. E. Kochevar, Spatially-Resolved Cellular Responses to Singlet Oxygen, *Photochem. Photobiol.*, 2006, **82**, 1178-1186.

15 L.-O. Klotz, K.-D. Kröncke and H. Sies, Singlet Oxygen-Induced Signaling Effects in Mammalian Cells, *Photochem. Photobiol. Sci.*, 2003, **2**, 88-94.

16 A. Blázquez-Castro, T. Breitenbach and P. R. Ogilby, Singlet oxygen and ROS in a new light: low-dose subcellular photodynamic treatment enhances proliferation at the single cell level., *Photochem. Photobiol. Sci.*, 2014, **13**, 1235-1240.

17 J. W. Snyder, E. Skovsen, J. D. C. Lambert, L. Poulsen and P. R. Ogilby, Optical Detection of Singlet Oxygen from Single Cells, *Phys. Chem. Chem. Phys.*, 2006, **8**, 4280-4293.

18 E. F. F. Silva, B. W. Pedersen, T. Breitenbach, R. Toftegaard, M. K. Kuimova, L. G. Arnaut and P. R. Ogilby, Irradiation- and Sensitizer-Dependent Changes in the Lifetime of Intracellular Singlet Oxygen Produced in a Photosensitized Process., *J. Phys. Chem. B.*, 2012, **116**, 445-461.

19 K. Tanaka, T. Miura, N. Umezawa, Y. Urano, K. Kikuchi, T. Higuchi and T. Nagano, Rational Design of Fluorescein-Based Fluorescence Probes. Mechanism-Based Design of a Maximum Fluorescence Probe for Singlet Oxygen., *J. Am. Chem. Soc.*, 2001, **123**, 2530-2536.

20 B. Song, G. Wang, M. Tan and J. Yuan, A Europium(III) Complex as an Efficient Singlet Oxygen Luminescence Probe, *J. Am. Chem. Soc.*, 2006, **128**, 13442-13450.

21 K. Xu, L. Wang, M. Qiang, L. Wang, P. Li and B. Tang, A selective near-infrared fluorescent probe for singlet oxygen in living cells, *Chem. Commun.*, 2011, **47**, 7386-7388.

22 R. Ruiz-Gonzalez, R. Zanocco, Y. Gidi, A. L. Zanocco, S. Nonell and E. Lemp, Naphthoxazole-Based Singlet Oxygen Fluorescent Probes, *Photochem. Photobiol.*, 2013, **89**, 1427-1432.

23 X. Li, G. Zhang, H. Ma, D. Zhang, J. Li and D. Zhu, 4,5-Dimethylthio-4'-[2-(9-anthryloxy)ethylthio]tetrathiafulvalene, a Highly Selective and Sensitive Chemiluminescence Probe for Singlet Oxygen, *J. Am. Chem. Soc.*, 2004, **126**, 11543-11548.

24 D. Song, S. Cho, Y. Han, Y. You and W. Nam, Ratiometric Fluorescent Probes for Detection of Intracellular Singlet Oxygen, *Org. Lett.*, 2013, **15**, 3582-3585.

25 S. K. Pedersen, J. Holmehave, F. H. Blaikie, A. Gollmer, T. Breitenbach, H. H. Jensen and P. R. Ogilby, Aarhus Sensor Green: A Fluorescent Probe for Singlet Oxygen, *J. Org. Chem.*, 2014, **79**, 3079-3087.

26 C. Schweitzer and R. Schmidt, Physical Mechanisms of Generation and Deactivation of Singlet Oxygen, *Chem. Rev.*, 2003, **103**, 1685-1757.

27 F. Wilkinson, W. P. Helman and A. B. Ross, Rate Constants for the Decay and Reactions of the Lowest Electronically Excited Singlet State of Molecular Oxygen in Solution. An Expanded and Revised Compilation., *J. Phys. Chem. Ref. Data*, 1995, **24**, 663-1021.

28 A. Kumagai, R. Ando, H. Miyatake, P. Greimel, T. Kobayashi, Y. Hirabayashi, T. Shimogori and A. Miyawaki, A Bilirubin-Inducible Fluorescent Protein from Eel Muscle, *Cell*, 2013, **153**, 1602-1611.

29 D. A. Lightner, T. A. Woolridge and A. F. McDonagh, Configurational Isomerization of Bilirubin and the Mechanism of Jaundice Phototherapy., *Biochem. Biophys. Res. Comm.*, 1979, **86**, 235-243.

30 L. Cheng and D. A. Lightner, A New Photoisomerization of Bilirubin, *Photochem. Photobiol.*, 1999, **70**, 941-948.

31 C. S. Foote and T.-Y. Ching, Chemistry of Singlet Oxygen. XXI. Kinetics of Bilirubin Photooxygenation., *J. Am. Chem. Soc.*, 1975, **97**, 6209-6214.

32 P. DiMascio, S. Kaiser and H. Sies, Lycopene as the Most Efficient Biological Carotenoid Singlet Oxygen Quencher., *Archives Biochem. Biophys.*, 1989, **274**, 532-538.

33 A. F. McDonagh, Turning Green to Gold, *Nature Structural Biology*, 2001, **8**, 198-200.

34 B. Greene, Picosecond Primary Photoprocesses of Bilirubin Bound to Human Serum Albumin, *Proc. Natl. Acad. Sci. USA*, 1981, **78**, 2008-2012.

35 T.-L. To, M. J. Fadul and X. Shu, Singlet oxygen triplet energy transfer-based imaging technology for mapping protein-protein proximity in intact cells., *Nature Comm.*, 2014, **5**, 4072.

36 J. H. Christensen, P. K. Hansen, O. Lillelund and H. C. Thøgersen, Sequence-specific binding of the N-terminal three-finger fragment of Xenopus transcription factor IIIA to the internal control regioon of a 5S RNA gene., *FEBS Lett.*, 1991, **281**, 181-184.

37 J. Arnbjerg, M. Johnsen, P. K. Frederiksen, S. E. Braslavsky and P. R. Ogilby, Two-Photon Photosensitized Production of Singlet Oxygen: Optical and Optoacoustic Characterization of Absolute Two-Photon Absorption Cross Sections for Standard Sensitizers in Different Solvents., *J. Phys. Chem. A*, 2006, **110**, 7375-7385.

38 P. Salice, J. Arnbjerg, B. W. Pedersen, R. Toftegaard, L. Beverina, G. A. Pagani and P. R. Ogilby, Photophysics of Squaraine Dyes: Role of Charge-Transfer in Singlet Oxygen Production and Removal., *J. Phys. Chem. A*, 2010, **114**, 2518-2525.

39 R. L. Jensen, J. Arnbjerg and P. R. Ogilby, Reaction of Singlet Oxygen with Tryptophan in Proteins: A Pronounced Effect of the Local Environment on the Reaction Rate., *J. Am. Chem. Soc.*, 2012, **134**, 9820-9826.

40 E. F. Pettersen, T. D. Goddard, C. C. Huang, G. S. Couch, D. M. Greenblatt, E. C. Meng and T. E. Ferrin, UCSF Chimera: A visualization system for exploratory research and analysis., *J. Comput. Chem.*, 2004, **25**, 1605-1612.

41 W. C. Johnson, Secondary Structure of Proteins Through Circular Dichrosim Spectroscopy, *Ann. Rev. Biophys. Biophys. Chem.*, 1988, **17**, 145-166.

42 I. Goncharova, S. Orlov and M. Urbanova, Chiroptical Propertiesof Bilirubin-Serum Albumin Binding Sites, *Chirality*, 2013, **263**, 257-263.

43 I. Goncharova, S. Orlov and M. Urbanova, The Location of the High- and Low-Affinity Bilirubin Binding Sites on Serum Albumin: Ligand-Competition Analysis Investigated by Circular Dichroism., *Biophys. Chem.*, 2013, **180-181**, 55-65.

44 D. A. Lightner, W. M. D. Wijekoon and M.-H. Zhang, Understanding Bilirubin Conformation and Binding: Circular Dichroism of Human Serum Albumin Complexes with Bilirubin and its Esters., *J. Biol. Chem.*, 1988, **263**, 16669-16676.

45 P. R. Ogilby, Solvent Effects on the Radiative Transitions of Singlet Oxygen, *Acc. Chem. Res.*, 1999, **32**, 512-519.

46 A. Gollmer, J. Arnbjerg, F. H. Blaikie, B. W. Pedersen, T. Breitenbach, K. Daasbjerg, M. Glasius and P. R. Ogilby, Singlet Oxygen Sensor Green®: Photochemical Behavior in Solution and in a Mammalian Cell., *Photochem. Photobiol.*, 2011, **87**, 671-679.

47 N. A. Kuznetsova, N. S. Gretsova, V. M. Derkacheva, S. A. Mikhalenko, L. I. Solov'eva, O. A. Yuzhakova, O. L. Kaliya and E. A. Luk"yanets, Generation of Singlet Oxygen with Anionic Aluminum Phthalocyanines in Water, *Russ. J. Gen. Chem.*, 2002, **72**, 300-306.

48 J. Davila and A. Harriman, Photoreactions of Macrocyclic Dyes Bound to Human Serum Albumin, *Photochem. Photobiol.*, 1990, **51**, 9-19.

49 M. J. Davies, Singlet Oxygen-Mediated Damage to Proteins and its Consequences., *Biochem. Biophys. Res. Comm.*, 2003, **305**, 761-770.

50 M. J. Davies, Reactive species formed on proteins exposed to singlet oxygen, *Photochem. Photobiol. Sci.*, 2004, **3**, 17-25.

51 F. M. Pimenta, R. L. Jensen, T. Breitenbach, M. Etzerodt and P. R. Ogilby, Oxygen-Dependent Photochemistry and Photophysics of "miniSOG", a Protein-Encased Flavin, *Photochem. Photobiol.*, 2013, **89**, 1116-1126.

52 P. Robertson and I. Fridovich, A Reaction of the Superoxide Radical with Tetrapyrroles., *Arch. Biochem. Biophys.*, 1982, **213**, 353-357.

53 E. R. Stadtman and R. L. Levine, Free Radical Mediated Oxidation of Free Amino Acids and Amino Acid Residues in Proteins., *Amino Acids*, 2003, **25**, 207-218.

54 C. C. Winterbourn, H. N. Parsons-Mair, S. Gebicki, J. M. Gebicki and M. J. Davies, Requirements for Superoxide-Dependent Tyrosine Hydroperpoxide Formation in Peptides, *Biochem. J.*, 2004, **381**, 241-248.

55 M. J. Davies, The Oxidative Environment and Protein Damage., *Biochem. Biophys. Acta*, 2005, **1703**, 93-109.

56 D. T. Sawyer, *Oxygen Chemistry*, Oxford University Press, New York, 1991.

57 B. Bielski, D. Cabelli, R. Arudi and A. Ross, Reactivity of HO_2/O_2 Radicals in Aqueous Solutions., *J. Phys. Chem. Ref. Data*, 1985, **14**, 1041-1101.

58 I. B. C. Matheson, N. U. Curry and J. Lee, Reaction Rate of Bilirubin with Singlet Oxygen and Its Strong Enhancement by Added Base., *J. Am. Chem. Soc.*, 1974, **96**, 3348-3351.

59 E. L. Clennan and A. Pace, Advances in Singlet Oxygen Chemistry, *Tetrahedron*, 2005, **61**, 6665-6691.

60 P.-G. Jensen, J. Arnbjerg, L. P. Tolbod, R. Toftegaard and P. R. Ogilby, Influence of an Intermolecular Charge-Transfer State on Excited-State Relaxation Dynamics: Solvent Effect on the Methylnaphthalene-Oxygen System and its Significance for Singlet Oxygen Production., *J. Phys. Chem. A*, 2009, **113**, 9965-9973.

61 P. Mukerjee and J. D. Ostrow, Interactions of unconjugated bilirubin with vesicles, cyclodextrins and micelles: New modeling and the role of high pKa values., *BMC Biochemistry*, 2010, **11**, 16.

62 R. D. Scurlock, M. Kristiansen, P. R. Ogilby, V. L. Taylor and R. L. Clough, Singlet Oxygen Reactions in a Glassy Polystyrene Matrix, *Polym. Degrad. Stab.*, 1998, **60**, 145-159.

63 J. R. Lakowicz and G. Weber, Quenching of Protein Fluorescence by Oxygen. Detection of Structural Fluctuations in Proteins on the Nanosecond Time Scale., *Biochemistry*, 1973, **12**, 4171-4179.

64 G. B. Strambini and P. Cioni, Pressure-Temperature Effects on Oxygen Quenching of Protein Phosphorescence, *J. Am. Chem. Soc.*, 1999, **121**, 8337-8344.

65 A. Jimenez-Banzo, X. Ragas, S. Abbruzzetti, C. Viappiani, B. Campanini, C. Flors and S. Nonell, Singlet Oxygen Photosensitization by GFP Mutants: Oxygen Accessibility to the Chromophore., *Photochem. Photobiol. Sci.*, 2010, **9**, 1336-1341.

66 R. Ruiz-Gonzalez, A. L. Cortajarena, S. H. Mejias, M. Agut, S. Nonell and C. Flors, Singlet oxygen generation by the genetically-encoded tag miniSOG, *J. Am. Chem. Soc.*, 2013, **135**, 9564-9567.

67 S. V. Lepeshkevich, M. V. Parkhats, A. S. Stasheuski, V. V. Britikov, E. S. Jarnikova, S. A. Usanov and B. M. Dzhagarov, Photosensitized Singlet Oxygen Luminescence from

the Protein Matrix of Zn-Substituted Myoglobin, *J. Phys. Chem. A*, 2014, **118**, 1864-1878.

68 R. A. Lundeen and K. McNeill, Reactivity Differences of Combined and Free Amino Acids: Quantifying the Relationship between Three-Dimensional Protein Structure and Singlet Oixygen Reaction Rates., *Environ. Sci. Technol.*, 2013, **47**, 14215-14223.

69 D. Voet and J. G. Voet, *Biochemistry*, John Wiley and Sons, New York, 2004.

70 N. A. Kuznetsova, N. S. Gretsova, O. A. Yuzhakova, V. M. Negrimovskii, O. L. Kaliya and E. A. Luk'yanets, New Reagents for Determination of the Quantum Efficiency of Singlet Oxygen Generation in Aqueous Media., *Russian J. Gen. Chem.*, 2001, **71**, 36-41.

71 V. Marx, Probes: seeing in the near infrared, *Nature Methods*, 2014, **11**, 717-720.

TOC Graphic

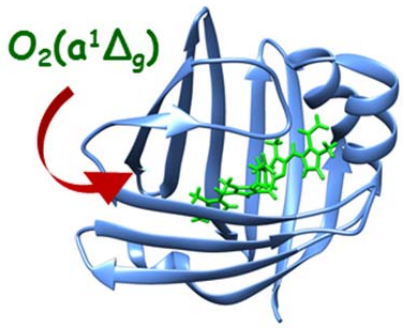

TOC Graphical Abstract

Oxygen- and singlet-oxygen-dependent parameters that characterize the behavior of bilirubin encapsulated in a protein have been quantified.